Bioengineering Research

Characterization and Biocompatibility of Hydroxyapatite Nanoparticles Extracted from Fish Bone

Esmaeil Biazar[1*], Morteza Daliri J[2], Saeed Heidari K[3], Dehghan Navayee A[4], Mahshad Kamalvand[1], MohammadAli Sahebalzamani[5], Faryma Royanian[1], Maryam Shabankhah[1], Fatemeh Farajpour L[1]

[1]Department of Biomaterials Engineering, Tonekabon Branch, Islamic Azad University, Tonekabon, Iran.
[2]Department of Animal Biotechnology, National Institute of Genetic Engineering and Biotechnology, Tehran, Iran.
[3]Department of Tissue Engineering, School of Advanced Technologies in Medicine, Shahid Beheshti University of Medical Sciences, Tehran, Iran.
[4]Biomaterial group, Faculty of New Sciences and Technologies, Semnan University, Semnan, Iran.
[5]Department of Biomaterials, Faculty of Biomedical Engineering, Science and Research, Branch, Islamic Azad University, Tehran, Iran.

Correspondence to: Biazar E. (kia_esm@yahoo.com.)

Abstract

In this study, hydroxyapatite (HAp) from fish bone was extracted by thermal calcination method, and then compared to chemical synthesized HAp. The samples were analyzed by Fourier Transform Infrared spectroscopy (FT-IR), X-Ray Diffraction analysis (XRD), Elemental analyze, Scanning Electron Microscopy, and cell tests. The FT-IR results showed well the presence of functional groups related to hydroxyapatite. The XRD results were in agreement with standard data. Size of the HAp Particle obtained about 300 and 50 nm for fish bone HAp and chemical synthesized samples, respectively. Good crystallinity and rod-like structures were showed for the fish bone HAp samples. The cell results with osteoblast-like cells showed well biocompatibility and proliferation of the cells on HAp nanoparticles. This study confirms that extracted fish bone is a promising biomaterial for bone regeneration.

Keywords: Hydroxyapatite (HAp), Fish bone, Sol-gel method, Characterization, Cell studies

Received: 9 May 2020, Accepted: 25 June 2020

DOI: 10.22034/jbr.2020.230516.1021

1. Introduction

Bone is a living tissue with hierarchical structure contains 70% calcium phosphate mostly nanoscale hydroxyapatite (HAp) crystals, and 30% organic materials including collagen, glycoproteins, proteoglycans, and sialoproteins by dry weight. Hydroxyapatite [HAp, $Ca_{10}(PO_4)_6(OH)_2$] is a type of calcium phosphates, which has opened an important role in the healing of hard tissues such as bone and tooth, due to biocompatibility and similar composition to natural bone [1-3]. In recent years, many progress has been made in the field of tissue regeneration, and the use of artificial prostheses to

treat the loss or failure of an organ or tissue [4-6]. Autograft and allograft have been considered as ideal techniques for bone grafting. Both of the techniques have showed some problems such as unwanted immunological responses and the risk of diseases transmissible by tissues and fluids [7, 8]. The Hap powders isolated from natural sources like cuttlefish bone [9], bovine bone [10-15] and fish bone [16-20] have showed an advantage of providing inexpensive raw materials from bone and teeth when compared to chemical synthesized HAp. Different methods have been applied to obtain nanometric HAp and properties similar to body bone HAp especially good biocompatibility [21-36]. In this paper, we produced and compared two type of the HAp extracted from fish bone and synthesized by sol-gel technique and studied different properties of the HAp nanopowders. Furthermore, their cytotoxicity has been studied with osteoblast-like MG-63 cell line.

2. Materials and Methods

2.1. Fish Bone Preparation

The fish bone (*Caspian kutum*) was washed and cleaned with hot water to remove the traces of meat and skin. The cleaned bones were mixed with 1.0% sodium hydroxide and acetone to remove protein, lipids, oils and other organic impurities (the bone and sodium hydroxide solid/liquid ratio was 1:50). After washing the bones were dried at 60 ºC for 24 h.

2.2. Thermal Method

The fish bones were placed in an oven and subjected to a temperature of 600 ºC with heating rate of 10 °C/min in an electrical muffle furnace in the presence of air atmosphere for 6 h, and then the samples were maintained isothermally for 6 h and cooled at oven. The calcined samples were milled by the use of milling balls.

2.3. Chemical method

The Hap nanoparticles was obtained using the sol-gel method with Ca $(NO_3)_2{\cdot}4H_2O$ and phosphoric acid (H_3PO_4) and ammonia (NH_3) as precursors (Eq.1). The phosphate solution (0.25 M) was added drop into the calcium containing solution (1M) with a magnetic stirrer. The ammonia was added and stirred till a constant pH=10 was obtained. The resultant mixture was stirred for additional 60 min for 24 h at room temperature. The obtained gel after aging was dried at 65°C for 24 h in a dry oven, and then washed repeatedly using double distilled water to remove $NH^{+}{}_{4}$ and $NO^{-}{}_{3}$. Finally, the powders were calcined in air at 600°C for 30 min using a heating rate of 10°C/min. [37].

(Eq.1)

$$H_3PO_4 + 3NH_4OH \rightarrow (NH_4)_3PO_4 + 3H_2O$$

$$6(NH_4)_3PO_4 + 10Ca\ (NO_3)_2{\cdot}4H_2O \rightarrow Ca_{10}(PO_4)_6(OH)_2 + 20NH_4NO_3$$

2.4. Characterization

The stretching frequencies of HAp samples were investigated by Fourier Transform Infrared spectroscopy (FT-IR) (BoMem Model MB100) within the range of 400 to 4000 cm^{-1}. The phase and crystallinity of the samples were evaluated X-ray diffraction (XRD) (Siemens and Bruker, Erlangen, Germany), with Cu-Kα radiation (range 5° to 70°). The phases were identified by comparing the experimental X-ray diffractions with the standard (Joint Committee on Powder Diffraction Standards (JCPDS09-0342/1996)). Size and morphology of the particles were studied by a Scanning Electron Microscope (SEM) (XL30; Philips, Eindhoven, Holland) equipped with Energy Dispersive Spectroscope (EDS) to analyze chemical composition. For cell analyses, the Human osteoblast-like MG-63 cell line (National Cell Bank(NCBI), Pasteur Institute, Iran) was cultured in DMEM/F12 medium supplemented with 10% fetal bovine serum, 1% penicillin/streptomycin, 1% L-glutamine, 1% NEAA (non-essential amino acids) and 1% pyruvate at 37 ºC under a humidified atmosphere containing

5% carbon dioxide. The samples were placed in Petri dishes using a sterilized pincer; 3 ml of the cell suspension was removed by pipette and poured into the control (TCPS; Tissue Culture Poly Styrene) and experimental samples. Thereafter, all of the samples were placed separately in a Memmert incubator at 37°C for 24 and 48 hours. The samples in the polystyrene Petri dish were removed from the incubator after 24 and 48 hours and studied using an Eclipse TS-100 photonic microscope (200X; Nikon, Tokyo, Japan). Cell viability was determined from measurement of the viable cell numbers by MTT assay [34]. The colorimetric measurement was performed at a wavelength of 570 nm using a microplate reader. All experiments were run in four replicates and the data were presented as the mean value ± standard deviation (SD) of each group. The samples with cells were washed by PBS, and then fixed by glutaraldehyde (2.5%) at 4°C for 2 hours. The samples were dehydrated by alcohols, and then kept with tetroxide osmium vapors at 4°C for 2 hours. The samples were kept in a desiccator, then coated with gold, and investigated by a SEM (Cambridge Stereo-scan, S-360).

Alkaline phosphatase activity was investigated using the method described by Miyajima [38]. Briefly, the powders at concentrations of 40 µg/ml with MG-63 cells for 10 days were washed twice with PBS before adding 150 ml pNPP substrate solution (Sigma, N2770). Enzyme activity was terminated by adding 38 ml 3M NaOH after 30 min incubation at 37 ºC. Alkaline phosphatase activity was then measured by the light absorbance observed at 405 nm from amount of the p-nitrophenol. All data are expressed as mean standard error of the mean unless noted (Student's t-tests were conducted with a significance level of $p<0.05$). A minimum of three replicate samples were used for all experiments.

3. Results and Discussion

The FTIR spectra from the calcined samples at 600 °C were presented in figure 1. The peaks 1093, 1047 cm^{-1} (fish bone HAp sample) and 1033 cm^{-1} (synthesized HAp sample) were related to PO_4^{3-} groups. Hydroxyl stretching mode was observed on all the samples at 3573 cm^{-1}. The presence of B-type carbonate hydroxyapatite in fish bone HAp sample was confirmed by FTIR spectra [39]. The carbonate ions were detected at 1640 to 1460 cm^{-1} in the fish bone HAp sample. The presence of organic material (CH) was detected as low intensity peaks at 2965 cm^{-1} for fish bone HAp sample. A weak band of CO_2^{3-} was detected in the region around 1465 cm^{-1}. It suggests small part of the PO_4^{3-} (B-type) groups in the apatite structure was replaced by CO_2^{3-}.

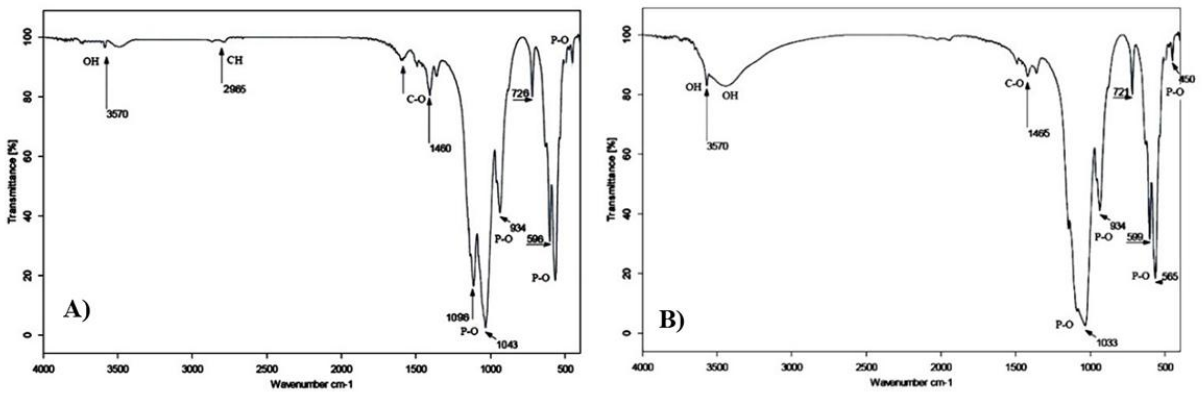

Figure 1. *FTIR spectra of the HAp extracted from fish bone (A), and chemical synthesized sample (B).*

The calcined powder at 600 °C consisted entirely of the HAp phase with well-defined peaks, as can be seen in figure 2, where the XRD patterns of the fish bone HAp sample were compared with chemical synthesized sample. In addition, there is no difference in the XRD patterns between the studied samples with standard peak.

The crystallite size of particles can be approximately calculated from the XRD patterns by Scherrer's equation (Eq.2) [35].

$$D = k\lambda / \beta\cos\theta \qquad \text{(Eq.2)}$$

Where D is the average dimension of crystallites in a direction normal to the diffracting plane *hkl*; β is the full width of the peak at half maximum intensity located at 2θ; λ is the wavelength of X-ray radiation and k is the Scherrer constant related to crystallite shape (Table 1).

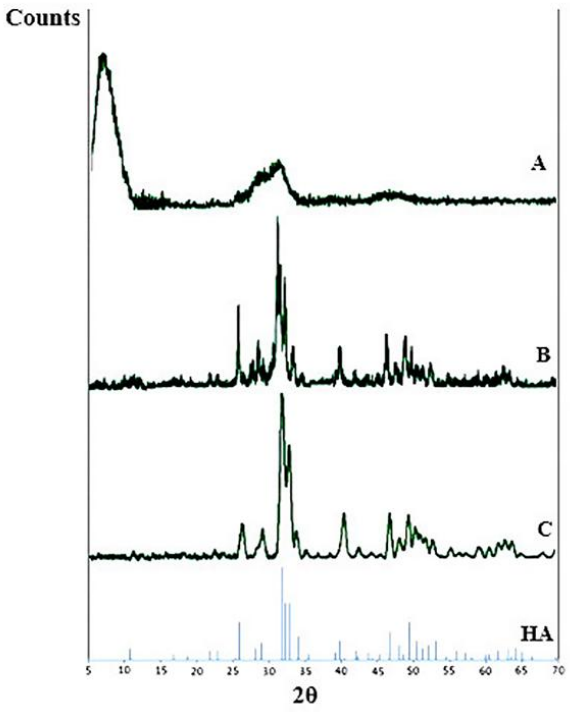

Figure 2. X-ray diffraction spectra of the raw bone (A), chemical synthesized HAp sample (B), HAp extracted from fish bone (C), and control (HA, JCPDS-09-0432) .

Table 1. FWHM of the (211) and average crystallite size of the HAp particles obtained from fish bone and chemical method.

Sample	FWHM of 211 peak 2Θ = 31.8	Crystal size (nm)
Fish bone	0.031	295±12
Synthesized HAp	0.175	54±31

Figure 3 showed morphologies of the HAp particles by SEM analysis. The images indicated that the particles are composed of rod-like shape particles with nanometric size. This rod-like shape can be attributed to the coupled CO_2^{-3} for PO_3^{-4} and Na^+ for Ca^{2+} substitutions that cause changes in morphology of the apatite crystals [40]. The average particle size of the HAp particles originated from the fish bones and the synthesized method were ~300 and 50 nm, respectively. Table 2 showed the EDS analysis of the extracted HAp which consisted of Oxygen (O), Phosphorous (P) and Calcium (Ca) atoms. The percentage atomic ratios of the Ca/P for the extracted HAp from fish bone, and the chemical synthesized samples were 1.82, and 1.68, respectively. The Ca/P ratios of the HAp extracted from fish bone was higher than those of the stoichiometric HAp, and these results are consistent with a previous report [40].

Table 2. Element content of the calcined HAp particles.

Sample	Atomic % Ca	P	O	Ca/P ratio
Fish bone	27.14	14.89	48.92	1.82
Synthesized HAp	16.33	9.72	50.45	1.68

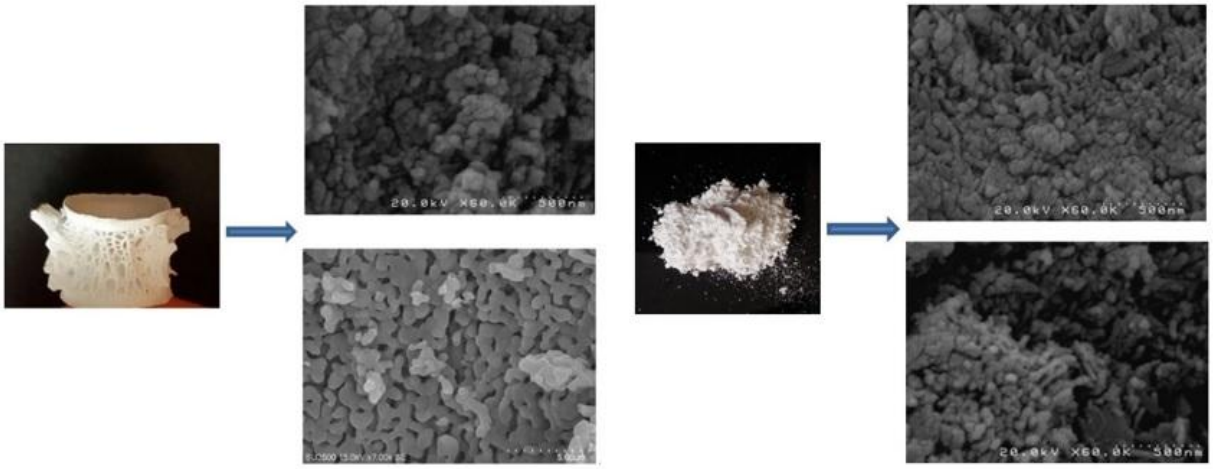

Figure 3. SEM images of the HAp samples extracted from fish bone (A), and chemical synthesized samples (B).

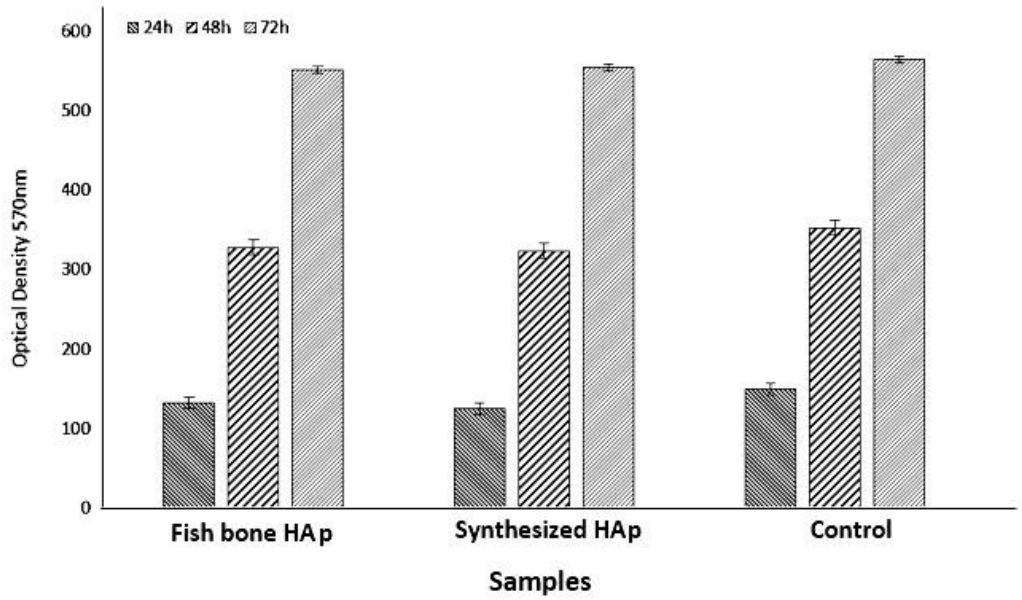

Figure 4. MTT assay for the hydroxyapatite extracted from fish bone, and chemical synthesized method. $P<0.05$.

Figure 4 showed cytotoxicity of the HAp particles. In the MTT assay the cells produced large amount of colored formazan that indicate all the tested powders are non-cytotoxic. None of the particles showed detrimental effect on cellular activity. The SEM images (Figure 5) also showed well cell attachment on the particles. It was observed that the HAp extracted from the fish bones (*Caspian kutum*) significantly promote the viability of osteoblasts. The CO_3^{2-} groups are beneficial to the cell adhesion and promote cell proliferation may likely explain the difference of the bioactivity of the HAp [41]. Therefore, the hydroxyapatite contained the CO_3^{2-} substitution especially in fish bone HAp exhibited higher biological activity.

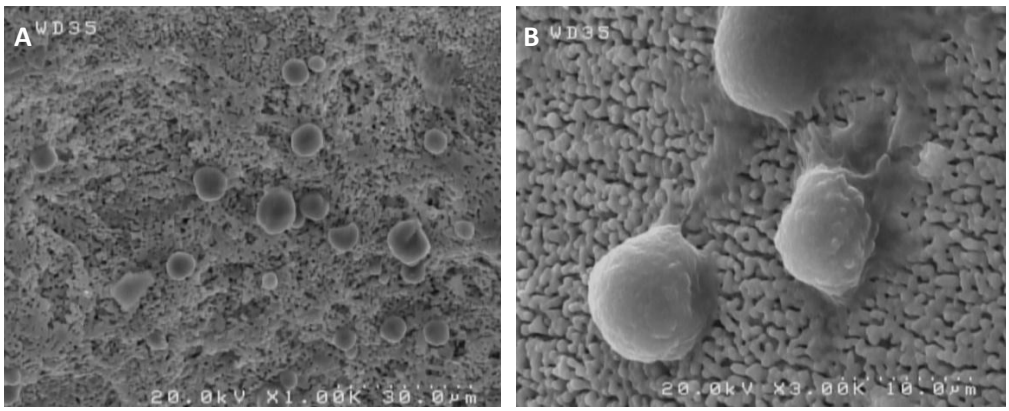

Figure 5. SEM images of the cultured cells on hydroxyapatite samples extracted from fish bone (A), and chemical synthesized method.

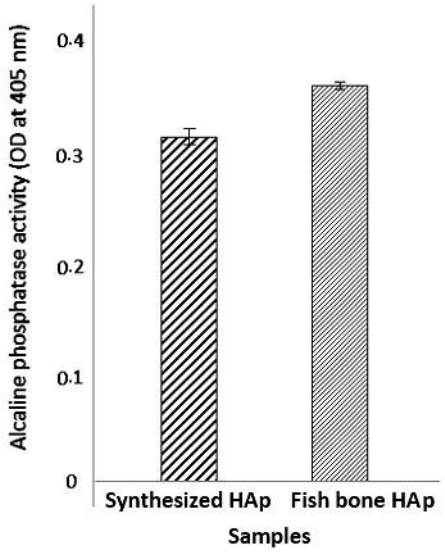

Figure 6. The alkaline phosphatase activity of the MG63 cells on the HAp powders after culturing for up to 10 days. $P<0.05$.

As an early marker of the osteoblast differentiation, the alkaline phosphate activity (ALP) in the MG63 cells culture was determined to investigate the function of the powders. Figure 6 showed the ALP activity of the cells cultured on the Hap particles. It was observed that the ALP activity of the MG63 cells on the fish bone HAp was a little higher than that of the chemical synthesized HAp during the 10 days culturing period, demonstrating that there are stronger interactions between the fish bone HAp-osteoblast as compared with the chemical synthesized HAp particles ($p<0.05$). Previous studies have showed that the physical structure such as the crystalline formation and also the presence of the mineral ions, such as CO_3^{2-}, Mg^{2+}, may stimulate cells proliferation, differentiation, adhesion, and formation of mineralized tissue [42,43].

4. Conclusion

Biological hydroxyapatite was extracted from fish bones and compared with synthetic hydroxyapatite produced by sol-gel method. The obtained powders especially the fish bone HAp showed presence of the functional groups related to HAp and also carbonate groups in structure that is similar to carbonate presence in human bone. The MTT test, microscopic images, and ALP activity confirmed that the fish bone HAp were non-cytotoxic and promoted cell activity. The fish bone hydroxyapatite can be as a promising alternative instead of the synthetic apatite due to cheap source and containing bone substitutes.

Conflict of interest

The authors certify that they have no affiliations with or involvement in any organization or entity with any financial interest, or non-financial interest in the subject matter or materials discussed in this manuscript. The authors alone are responsible for the content and writing of the paper.

Acknowledgments

No applicable.

References

[1] Biazar E., Heidari Keshel S., Rezaei Tavirani M., Jahandideh R., Bone reconstruction in rat calvarial defects by chitosan/hydroxyapatite nanoparticles scaffold loaded with unrestricted somatic stem cells. Artificial Cells, Nanomedicine, and Biotechnology., 2015; 43: 112–116.

[2] Suchanek W., Yoshimura M., Processing and properties of hydroxyapatite-based biomaterials for use as hard tissue replacement implants. J Mater Res., 1998; 3: 94–117.

[3] De Lange GL., Donath K., Interface between bone tissue and implants of solid hydroxyapatite or hydroxyapatite-coated titanium implants. Biomaterials., 1989; 10: 121– 125.

[4] Horwitz EM., Prockop DJ., Fitzpatrick LA., Koo WW., Gordon PL., Neel M., et al., Transplantability and therapeutic effects of bone marrow-derived mesenchymal cells in children with osteogenesisimperfect. Nat Med., 1999; 5: 309– 313.

[5] Monteiro BS., Argolo-neto NM., Nardi NB., Treatment of critical defects produced in calvaria of mice with mesenchymal stem cells. An Acad Bras Cienc., 2012; 84: 841–851.

[6] Branski LK., Gauglitz GG., Herndon DN., Jeschke MG., A review of gene and stem cell therapy in cutaneous wound healing. Burns., 2009; 35: 171 – 180 .

[7] Giannoudis P., Dinopoulos H., Tsiridis E., Bone substitutes: an update. Injury., 2005; 36: 20–27.

[8] Langer R., Vacanti J., Tissue engineering. Science., 1993; 260: 920–926.

[9] Ivankovic H., Gallego Ferrer G., Tkalcec E., Orlic Sand Ivankovic M., Preparation of highly porous hydroxyapatite from cuttlefish bone. J. Mater. Sci.-Mater. Med., 2009; 20: 1039–1046.

[10] Barakat NAM., Khil MS., Omran AM., Sheikh FA., Kim HY., Extraction of pure natural hydroxyapatite from the bovine bones bio waste by three different methods. J. Mater. Process. Technol., 2009; 209: 3408–3415.

[11] Joschek S., Nies B., Krotz R., G¨opferich A., Chemical and physicochemical characterization of porous hydroxyapatite ceramics made of natural bone. Biomaterials., 2000; 21: 1645–1658.

[12] Ooi CY., Hamdi M., Ramesh S., Properties of hydroxyapatite produced by annealing of bovine bone.Ceram. Int., 2007; 33:1171–1177.

[13] Haberko K., Bucko M., Brzezinska-Miecznik J., Haberko M., Mozgawa W., Panz T., et al., Natural hydroxyapatite—its behaviour during heat treatment. J. Eur.Ceram. Soc., 2006; 26: 537–542.

[14] Haberko K., Bucko M., Haberko M., Mozgawa W., Pyda A., Zarebski J., Natural hydroxyapatite—preparation and properties. Eng Biomater., 2003; 6: 32–37.

[15] L¨u X., Fan Y., Gu D., Cui W., Preparation and characterization of natural hydroxyapatite from animal hard tissues. Key Eng. Mater., 2007; 342: 213–216.

[16] Coelho T., Nogueira E., Weinand W., Lima W., Steimacher A., Medina A., et al., Thermal propertiesof natural nanostructured hydroxyapatite extracted from fishbone waste. J. Appl. Phys., 2007; 101: 084701.

[17] Ozawa M., Satake K., Suzuki R., Removal of aqueous chromium by fish bone waste originated hydroxyapatite. J. Mater. Sci. Lett., 2003; 22: 513–514.

[18] Ozawa M., Suzuki S., Microstructural development of natural hydroxyapatite originated from fish-bone waste through heat treatment. J. Am. Ceram. Soc., 2002; 85: 1315–1317.

[19] Prabakaran K., Rajeswari S., Development of hydroxyapatite from natural fish bone through heat treatment .Trends Biomater. Artif. Organs., 2006; 20: 20–23.

[20] Venkatesan J., Kim SK., Effect of temperature on isolation and characterization of hydroxyapatite from tuna (Thunnus obesus) bone. Materials., 2010; 3: 4761–4772.

[21] Sahebalzamani M., Biazar E., Shahrezaei M., Hosseinkazemi H., Rahiminavaie H., Surface modification of PHBV nanofibrous mat by laminin protein and its cellular study. Int. J. Polym Mater Po., 2015; 64:149-154.

[22] Sahebalzamani A., Biazar E., Modification of poly caprolactone nanofibrous mat by laminin protein and its cellular study. J. Biomater. Tissue Eng., 2014; 4:423-429.

[23] Baradaran-Rafii A., Biazar E., Heidari-keshel S.,Cellular Response of Limbal Stem Cells on PHBV/Gelatin Nanofibrous Scaffold for Ocular Epithelial Regeneration. Int. J. Polym Mater Po., 2015; 64:879-887.

[24] Baradaran-Rafii A., Biazar E., Heidari-keshel S., Cellular Response of Stem Cells on Nanofibrous Scaffold for Ocular Surface Bioengineering. ASAIO J., 2015; 61: 605-612.

[25] Baradaran-Rafii A., Biazar E., Heidari-keshel S., Cellular Response of Limbal Stem Cells on Polycaprolactone Nanofibrous Scaffolds for Ocular Epithelial

Regeneration.Curr Eye Res., 2016; 41: 326-333.

[26] Biazar E., Heidari S., Sahebalzamani A., Hamidi M., Ebrahimi M., The healing effect of unrestricted somatic stem cells loaded in nanofibrous Polyhydroxybutyrate-co-hydroxyvalerate scaffold on full-thickness skin defects. J Biomater Tiss Eng., 2014; 4: 20-27.

[27] Keshel HS., Biazar E., Rezaei Tavirani M., Rahmati Roodsari M., Ronaghi A., Ebrahimi M., et al. The healing effect of unrestricted somatic stem cells loaded in collagen-modified nanofibrous PHBV scaffold on full-thickness skin defects. Artif. Cell. Nanomed B., 2014; 42:210-216.

[28] Biazar E., Heidari S., Effects of chitosan cross linked nanofibrous PHBV scaffold combined with mesenchymal stem cells on healing of full-thickness skin defects. J.Biomed Nanotechnol., 2013; 9:1471-1482.

[29] Biazar E., Khorasani MT., Montazeri N., Poorshamsian K., Daliri M., Rezaei M., et al., Types of neural guides and using nanotechnology for peripheral nerve reconstruction. Int.J.Nanomed., 2010; 5:839–852.

[30] Ameri R., Biazar E., Development of oriented nanofibrous silk guide for repair of nerve defects. Int. J. Polym Mater Po., 2016; 65: 91-95.

[31] Biazar E., Heidari SK., Chitosan-Cross-linked nanofibrous PHBV nerve guide for rat for sciatic nerve regeneration across a defect bridge. ASAIO J., 2013; 59: 651-659.

[32] Biazar E., Heidari S., Gelatin-Modified Nanofibrous PHBV Tube as Artificial Nerve Graft for Rat Sciatic Nerve Regeneration. Int. J. Polym Mater Po., 2014; 63: 330-336.

[33] Biazar E., Heidari S., Rat sciatic nerve regeneration across a 30-mm defect bridged by a nanofibrous PHBV and Schwann cell as artificial nerve graft. Cell Commun. Adhes., 2013; 20: 41-49.

[34] Biazar E, Keshel SH., Rezaei Tavirani M., Jahandideh R., Bone formation in calvarial defects by injectable nanoparticular scaffold loaded with stem cells. Expert Opin. Biol. Ther., 2013; 13: 1653-1662.

[35] N Montazeri., R Jahandideh., Biazar E., Synthesis of fluorapatite–hydroxyapatite nanoparticles and toxicity investigations. International Journal of Nanomedicine., 2011;6: 197–201.

[36] Ai J., Rezaei-Tavirani M., Biazar E., Keshel SH., Jahandideh R., Mechanical Properties of Chitosan-Starch Composite Filled HydroxyapatiteMicro- and Nanopowders Journal of Nanomaterials., 2011; 2011: 1-5. doi:10.1155/2011/391596.

[37] Sanosh KP., Chu MC., Balakrishnan A., Kim TN., Cho SJ., Preparation and characterization of nano-hydroxyapatite powder using sol–gel technique. Bull. Mater. Sci., 2009; 32: 465–470.

[38] Miyajima K., Effects of periodic tension on osteoblast-like cells for cell differentiation and alkaline phosphatase activity. Nippon Kyosei ShikaGakkai Zasshi. 1990;49 (3):226–236.

[39] Le Geros RZ., Le Geros JP., Dens Hydroxyapatite. in An introduction to Bioceramics, Hench LL., Wilson J., Eds. World Scientific, Singapore, 1993; 139–180.

[40] Boutinguiza M., Pou J., Comesaña R., Lusquiños F., de Carlos A., León B.,

Biological hydroxyapatite obtained from fish bones. Materials Science and Engineering C., 2012; 32: 478–486.

[41] Haberko K., Bućko MM., Brzezińska-Miecznik J., Haberko M., Mozgawa W., Panz T., et al., Natural hydroxyapatite—its behaviour during heat treatment. Journal of the European Ceramic Society., 2006; 26: 537-542.

[42] Shibata H., Yokoi T., Goto T., Kim IY., Kawashita M., Kikuta K., et al., Behavior of hydroxyapatite crystals in a simulated bodyfluid: effects of crystal face. Journal of the Ceramic Society of Japan., 2013; 121: 807-812.

[43] Toppe J., Albrektsen S., Hope B., Aksnes A., Chemical composition, mineral content and amino acid and lipid profiles in bones from various fish species. Comparative Biochemistry and Physiology Part B: Biochemistry and Molecular Biology., 2007; 146: 395-401.